MICROSTRUCTURE AND TRIBOLOGICAL CHARACTERISTICS OF BIOCOMPATIBLE 316 L STAINLESS STEEL

PhD physicist FLORINA VIOLETA ANGHELINA[1], PhD Eng. VASILE BRATU [1]

[1]Valahia University of Targoviste, Faculty of Mechanical and Materials Engineering, 130024, Targoviste, Romania
vianghelina@yahoo.com ; v_bratu22@yahoo.com

Abstract. *This paper reports the outcome of morphological and microcompozitional (SEM, EDS, X-Ray Maps, Compo and Morpho images) and tribological investigations of biocompatible 316 L stainless steel. The most important conclusion that can draw based on optical microscopy observations is that sparked-in morphology differs depending on its place on the surface of the same sample. This is given by point-to-plate geometry that favors central discharges and a specific sample erosion/etching.*
Keywords*: 316 L Stainless Steel , EDS, X-Ray Maps, Compo and Morpho Image, Tribological characteristics.*

1. Introduction

The 316L steel was created in the 1950s by reducing the carbon content from 0.08% to 0.03% in order to better corrosion resistance. Type 316L steel is steel sheets, strips, plates, standardized according to ASTM A240.
The outdoor melting steel 316L can lead to contamination and, in consequence, of low biocompatibility characteristics. For this reason we prefer 316LVM steel, low carbon steel melted in vacuum. A steel 316L or 316LVM is considered biocompatible if it satisfies ASTM F 138 or ISO 5832-1.

Table 1. **Chemical composition requirements, comparative presentation standards AISI, ASTM, ISO:**

Element	AISI max%	ASTM max%	ISO max%
C	0,03	0,03	0,03
Mn	2,0	2,0	2,0
P	0,045	0,025	0,025
S	0,03	0,01	0,01
Silicon	0,75	0,75	1,0
Cr	16,0-18,0	17,0-19,0	17,0-19,0
Ni	10,0-13,0	14,0-15,0	14,0-15,0
Mo	2,0-3,0	2,25-3,0	2,25-3,5
N	0,1	0,1	0,1
Co	not required	0,5	0,5
Fe	residue		

Table 2. Minimum mechanical properties required by ASTM A 240 and ASME SA-240:

Properties	Minimum mechanical properties required by ASTM A 240 and ASME SA-240	
	316	316L
Yield Strength 0,2% offset psi (MPa)	30 (204)	25 (170)
Tensile strength psi (MPa)	75 (515)	70 (485)
Elongation at 51 mm	40	40
Maximum hardness Brinell (RB)	217 (95)	217 (95)

Steels type AISI 316 L is a special type of biocompatible material for applications in orthopedics, to obtain which were done extensive research at SC COST SA Targoviste, Valahia University of Targoviste and Polytechnic University of Bucharest. In this case, questions have arisen about compositional analysis with high accuracy to validate their application in clinical practice. [1÷11].

2. Materials and methods

Optical emission spectrometry with spark excitation (OES-Spark Stand)

If using high energy discharge in argon atmosphere, a portion of the sample is remelted. The discharge vaporizes only a segment of the sample. The result of the analysis is independent of sample fragment structure remained.

The method technique known as HEPS (High Energy Pre Spark) allows calibration with reference materials and / or samples of materials with unknown structures.

With this technique you can obtain sufficiently accurate results making some corrections.

Detection limits for some elements (eg. Pb, Sb, Bi) require improvements.

OES method is complicated and requires a lot of time and abrasive paper. When using standard samples OES analysis for the elements Cr and Ni can record accuracy (2 S)> 1% rel For the spectrochemical test was used Specrolab spectrometer. To clear image of electric spark discharge in argon were investigated both macrostructural and microstructural optical microscopy and electron microscopy, SEM-EDS, sparking areas resulting from OES investigations method and associated studied samples of AISI 316L steel.

Determination of microstructure was performed in the laboratory of microstructural analysis of SC COST Targoviste, the laboratory is equipped with line type BUEHLER metallographic sample preparation. Microstructures were visualized with a microscope type REICHERT Univar assisted by a computer equipped with image analysis software.

The device is equipped with a high resolution digital camera Type Polaroid DMC 1E type TWAIN driver. Image analysis equipment, has a Frame Grabber type Matrox Meteor II. For SEM investigation of fingerprint evidence spark steel AISI 316L was used electron microscope XL-30-ESEM TMP equipped with ED-RS spectrometer (Fig. 1).

Fig. 1. Overview of electron microscope. XL-30-ESEM TMP.

The microscope is equipped with appropriate software to support the operation, data acquisition and processing of results ie SEM images, ED-XRF spectra etc. (Environmental Scanning Electron Microscope) [12].

Preparation of samples.

The samples studied are cylindrical samples (wires) that can be analyzed directly using a special support.

Armed with several standard samples first thing we must ensure is that the standards used are similar samples to be analyzed. The more similar in terms of compositional calibration will be even better. When using the technique HEPS sample preparation method has no influence on spectrochemical results as long as the chemical composition of the sample is changed. It takes into account possible decarburization evidence by overheating (cutting or crushing) and chopped material contamination.

Regarding electric discharge spark OES spectrometry used, it is considered that it would have a temperature of about 30 000 K, which would allow instant vaporization of the material from the discharge. Also, it is known that the electric discharge is primed metallic inclusions in the sample, formed by particles of slag, abrasive particles of the compound or at "paper" eg grinding. corrundum.
If the spectrometer was calibrated using standard samples unknown test results (especially for the elements precipitated) are valid when the intensities are measured at steady state. Specific times corresponding pre-spark samples are as follows:
For the control samples taken from the melt (steel, bio, and so on) that S <0.05%, pre-spark times are about 5 seconds.
To control the melt samples (steel casting), S <0.05% rise times of about 10 s
For samples of semi-finished and finished products with S <0.1% during the pre-spark is about 15 seconds.

3. Results and discussions.

3.1. Spectrometric analytical results.

Reproducibility of homogeneous samples obtained at different levels of concentrations can be compared with standard data BEC (Background Equivalent Concentration) and depending on the type of item [10,11].

Element type	Sample	Concentration 5>Bec	Concentration BEC
soluble	Cr, Ni, Mo,Cu	0,3-0,8	1-2
partially precipitated	Al, Ti, P	1-2	2-4
precipitate	S, As, Pb, Sb	2-4	4-8

It is impossible to make a classification of all elements as separate conditions of the elements depend on the presence or absence of other elements (oxides, carbides, sulfides) and also depend on the speed of cooling and deformation.
Calibration curves for C, Cr, Ni are typical of Cr and CrNi steels base.
Surface composition is interpreted by registering ratio metal / oxide for Cr and Fe. To measure the passivation, is determined the composition according to the depth, so the majority elements and for those who are in a lower proportion.
Below are presented the analysis of alloy 316L, polished mechanically and passivated respectively.

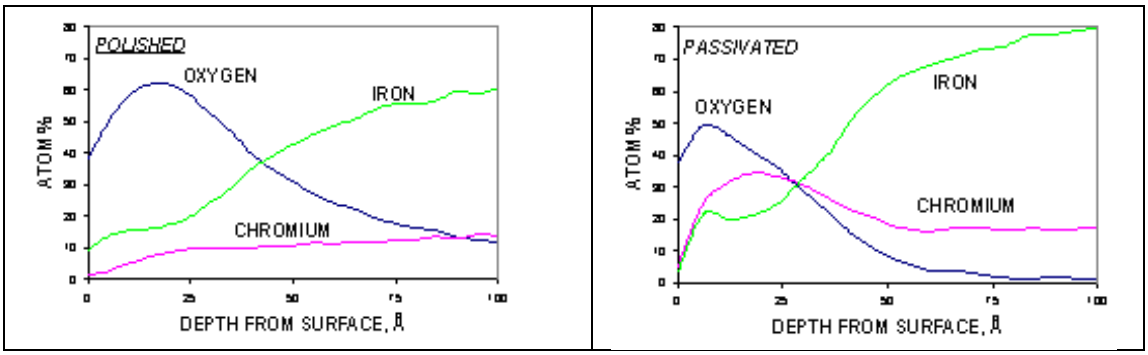

Fig 2.a Fig 2.b

Figure 2a presents the concentration of the elements O, Fe, Cr depending on the depth.
In Figure 2.b passivation effect is presented aiming at the report Cr / Fe.

3.2. Their macro and microscopic investigation of areas spark 316L steel samples. Macrostructural investigations.

Macroscopic images of the spark areas are shown in Fig.3. a, b.
Sample circled in Fig. 3.b was chosen to be investigated by metallographic microscopy and SEM-EDS microscopy. The sample shows four well differentiated sparks that are representative of the spark.


a)

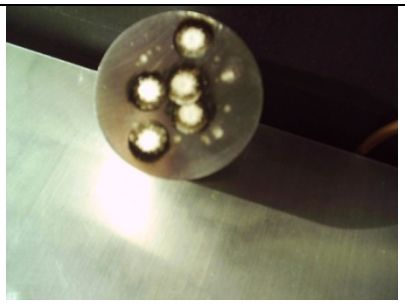
b)

Fig. 3. a) Macroscopic images of samples spark b) detail view.

Investigation metallographic microstructure by optical microscopy.
Microscopic investigation spark area. No 1.

The image of Fig. 4 presents the overall appearance of the surface spark. For granular appearance of the central area, which is different from the rest of the surface, it is possible to estimate the diameter of the spark. But this is not relevant from the point of view of accuracy, because there is a transition area from the scanned area of the surrounding area which has a diffuse and a non-homogeneous distribution of the incidence of sparks. The picture shows aspects that suggest the existence of pores or pitting in the spark sites. Also in Fig.4 demonstrates unmistakably that the sparked area is not uniformly morphological aspect uniformly .


Fig. 4. Overview of the sparkle area no. 1 (spark 1-1X)


Fig. 5. Overview of the central sparkle area no.1(spark 1-4X).

In the Fig.5 morphological aspects of the sparkle area are shown (spark 1). And this picture shows a granular morphology inhomogeneous local but homogeneous at zonal respectively grainy central area is homogenous relief tenths of a millimeter scale.

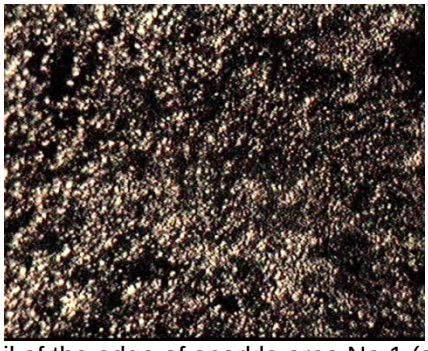
Fig..6. Detail of the edge of sparkle area No.1 (spark 1-4X)

The image transition area (Fig. 6) has a rougher than that of the morphology of the the central, which may be corroborated with the relevant aspects of Fig. 4

The most important aspect is metallographic microscopy revealed granular appearance, coarser, the center of the the spark in relation to adjacent areas. On the other hand, observing with the naked eye sparks suggests that marginal sparkle areas are rough.

Investigations by scanning electron microscopy.
As a result of investigations by optical microscopy, they do not get enough accurate information or covers to elucidate the mechanisms of interaction of spark sample steel AISI 316 L, therefore it was felt that an investigation by scanning electron microscopy as superior optical microscopy investigations. To highlight the microstructure at magnifications of 1500 - 2000X, the most used method is scanning electron microscopy (Scanning Electron Microscope - SEM).
The sample was subjected to investigation is sparkle area No.1, Overview of the sparkle zone obtained in the secondary electron (SE Secondary Electrons) is shown in Fig. 7.

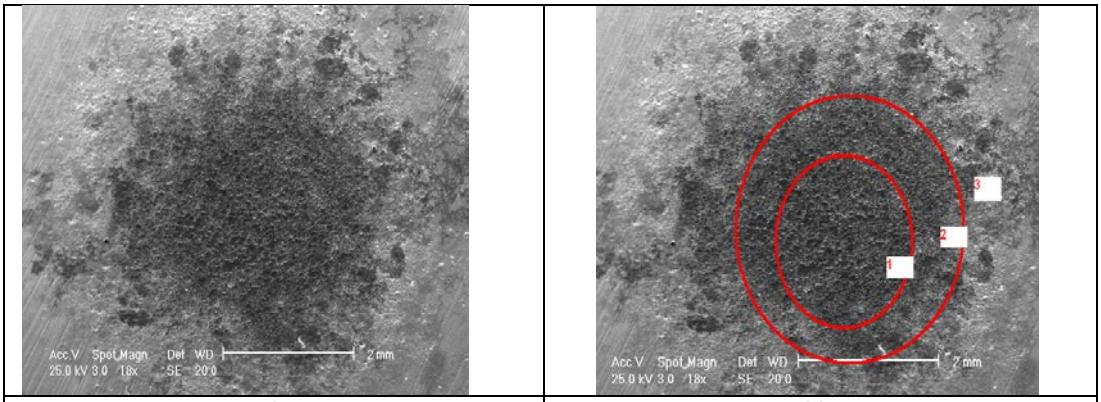

a) b)

Fig.7 Overview of the sparkle footprint) image markers b).

4. Conclusions.
Conclusions on investigations of samples of AISI 316L by metallographic microscopy.
Images spark one central areas suggest a texture attack (Fig. 9 5). Images peripheral areas, of the sparkle area, scattering sparks point out the existence of cracking the "field" full attack, but with less intensity. Explanation could be a net shaped spark, something like a jet shower, which has a significant scattering droplets of water that the incidence of a sand layer generates a small board crevice excavation. Similarly, it can be shown schematically, the morphological profile generated by a spark (Fig. 8).

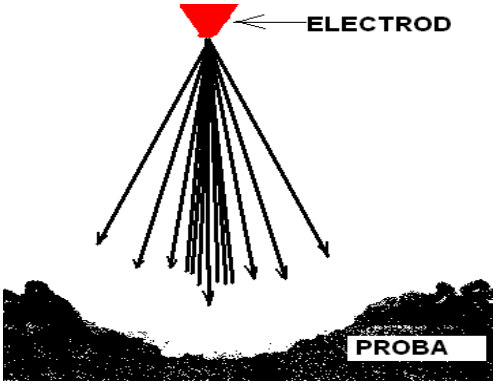

Fig. 218 Schematic representation the mode to "attack of sparks".

Thus, in Fig.9 is present unprocessed image of the central area of sparkr no. 1. This image was the "signal" input for frame Graber program that attempted to identify distinct structural units based on gray scale uniformity and discrimination of the threshold ("thre shoulding").

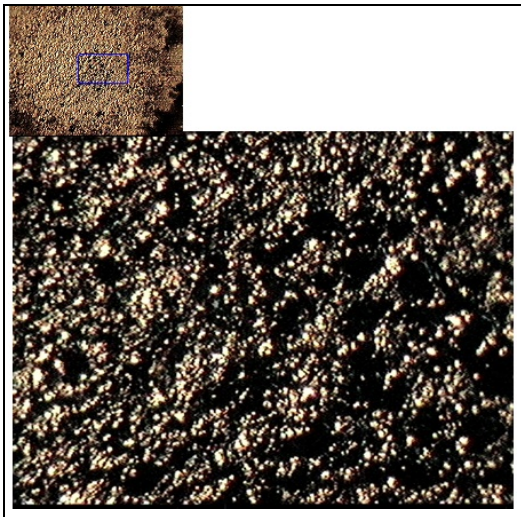

Fig..9 Raw image of the central area, the spark. 1

Analysis Statistics	Phase Area	Area (μm)
Minimum	18.606%	12.90532
Maximum	81.394%	2959.621
Mean	N/A	167.7805
Std. Dev.	N/A	261.7775
Field Statistics		
Total Scanned Area	1784032	
Field Area	1784032	
Number of Fields	1	

Tabelul 3. Data related to the image of Fig. 9

Results "structural discrimination / morphological" are given in Table 3. Thus, there are morphological discrimination unit, the minimum area of 13 μm^2 with a weight ratio of about 19% of the area under investigation and the maximum structural unit of area of about 300 μm^2 in a proportion of about 81%. Thanks the rough form of relief sample and lack of discrimination of thresholds, it is understandable that the data in Table 3 are not exact, but guidance. Detailed analysis of the image of semicentral fingerprint area no. 1 reveals that there is a small gradient transition intensity of the attack, from the center to the periphery.

Conclusions on investigations steel AISI 316 L samples by electron microscopy.

Of Fig. 7 make clear the overall morphology of the fingerprint spark, that is, it consists of a central location approximately circular (Fig. 417 b), in which the incidence of sparks (individual) to destroy preexisting structure. The area looks like a muddy field into the was raining with stone. This area has a diameter of about 2 mm. Circumscribing the disc is a ring, with the side of about 1 mm (Fig. 41.7 b), in which the incidence of spark bombardment is reduced, however, this crown are the recesses (pitting and crevice s) for which genesis can be assigned to most likely, discharge channels "fixed".

Backscatter electron images obtained are intended to highlight the heterogeneous chemical comoziţia the area concerned.

COMPO image of Fig.10 followed also highlight possible changes in the distribution of chemical elements into spark area. This picture does not reveal any significant inhomogeneities of chemical composition, but show morphological differences diminish due to the way of obtaining the SEM image.

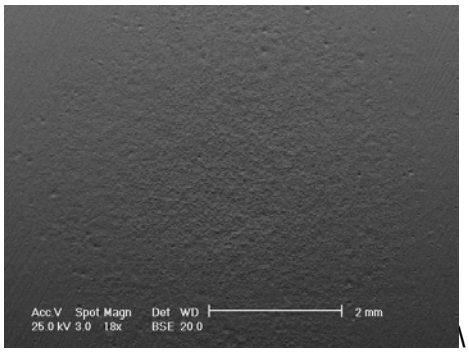

Fig.10 COMPO image of footprint spark.

In conclusion, BSE and COMPO images without relevant information in this case.

Elemental analysis to energy dispersive radiation spectrometry (ED-XRS-Energy Dispersion X-ray Spectroscopy-) can be correlated with BS and COMPO investigations to estimate the combined

effect of composition, segregation, or distillation of the elements into the sparkle surface. Therefore it was decided that the areas to be analyzed and investigated SEM ED-XRS. Thus, in Fig.11 presented the X-ray emission spectrum characteristic electron beam induced incidents. Of Fig. 11, that in the spark are found all main alloying elements in steel AISI 316 with intensities proportional to the concentrations of those elements.

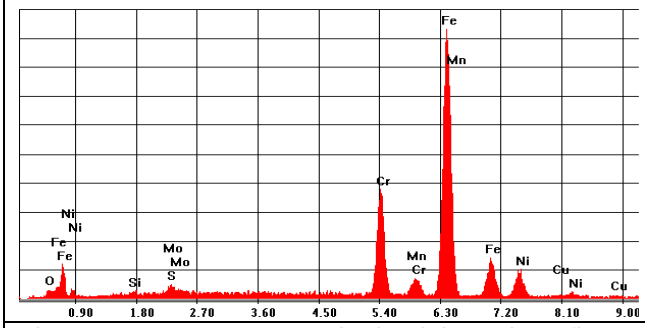

Fig.11 ED-XRF spectrum obtained throughout fingerprint of the spark

Element	C(%)
Cr	17,32
Ni	10,07
Mo	1,39
Mn	1,26
Si	0,62
Cu	1,3
O	2,34
S	0,42
Fe	65,28
Total	100

Tabel 4. The concentrations associated Fig. 11

Mass concentration C (%) dosed by ED-XRS technique corresponding of spectrum for Fig.11 is given in Table 4. All the evidence we experience light and electron microscopy SEM lead to the idea of a local discharge. Discharges are made through "channels" with relatively large diameters >2 μm, which remains to explain. A discharge channel generates shock waves that expels material as excited atoms, ions, and clusters and particles with diameter < 2 μm.
The particles are deposited on the periphery spark and generates a surface appearance to "peach skin".
"Peach skin" is the reason why the crown spark appears as black. In fact the crown contains nothing that has black or absorb light, but light is dispersible, or better said is scattered randomly scattered on the incidence at surface with the scattering centers at 0,2÷5 μm that break wavefront.
Basically, in the footprint, from the center outward diffusive particle density increases (which break wavefront incident) and practically no longer reflects light. What happens at this level remains to be studied! The fact is that black appearance, the appearance of smoked spot from the center to the interior, is given by metal particles deposited.
On the other hand, the center of the sample reflected light as the this smooth area, the sizes of 100-200 μm forming tiny mirrors that reflect the light diffusely. Thus, these investigations found the explanation of black crown spark zone, corresponding samples biocompatible steel AISI 316L.

REFERENCES.

[1].Constantin Baciu, ş.a.,"*Ştiinţa materialelor metalice"*, Ed.Didactică şi pedagogică R.A., Bucureşti,1996.
[2].Ghe.Ioniţă ş.a.,"*Evoluţia şi proprietăţile materialelor"*, Ed. Fundaţia "Metalurgia Română", Bucureşti,1998.
[3]. SR ISO 5832-1:1999, *Implanturi chirurgicale. Produse metalice. Partea 1: Oţel inoxidabil deformabil.*
[4]. Pencea I, *Bazele incercarilor spectrochimice de emisie optica prin scanteie si arc electric*, Ed. Printech, 2007.
[5]. B.Antoszewski, s.a., *A study of friction of textured surface,* Hidraulica Nr. 1 (23) /martie 2009.
[6]. Ilare BORDEAŞU, Ion MITELEA, Mircea Octavian POPOVICIU, Marcela SAVA, *Stainless steel cold-work hardening through cavitation* , ISSN 1453 – 7303 HIDRAULICA (No. 2/2013),Magazine of Hydraulics, Pneumatics, Tribology, Ecology, Sensorics, Mechatronics.
[7]. **A. Nocivin, I. Ciuca, *Guide Book of Metallic Biomaterials*, litografia UPB, 1998.
[8]. L.B.Loeb,*Statistical factors in spark discharge mechanisms*, Rev.Modern Phys. V. 20. No.1,p.151—160, 1948.
[9]. A. Jantschi, *Chimie Fizică. Analize Instrumentale*, Ed. AcademicDirect, 2004,
[10] I. Pencea, M. Branzei, F. Miculescu, M.Pencea, O.Trante, M. Miculescu, *The matrix effect on spectrochemical analysis accuracy of AISI 316 biomaterial grades*, Journal of optoelectronics and advanced materiales, v.9, No.11, November 2007, p. 3411 – 3414.
[11]. Contract CEEX 223/2006, *Materiale noi biocompatibile pentru implantologie ortopedica.*
[12] www.thermofisher.com/.